

# Inhibition of GAPDH activity by poly(ADP-ribose) polymerase activates three major pathways of hyperglycemic damage in endothelial cells

See the related Commentary beginning on page 986.

Xueliang Du,<sup>1</sup> Takeshi Matsumura,<sup>1</sup> Diane Edelstein,<sup>1</sup> Luciano Rossetti,<sup>1</sup> Zsuzsanna Zsengellér,<sup>2</sup> Csaba Szabó,<sup>2,3</sup> and Michael Brownlee<sup>1</sup>

<sup>1</sup>Diabetes Research Center, Albert Einstein College of Medicine, Bronx, New York, USA

<sup>2</sup>Inotek Pharmaceuticals, Beverly, Massachusetts, USA

<sup>3</sup>Institute of Human Physiology and Clinical Experimental Research, Semmelweis University, Budapest, Hungary

In this report, we show that hyperglycemia-induced overproduction of superoxide by the mitochondrial electron transport chain activates the three major pathways of hyperglycemic damage found in aortic endothelial cells by inhibiting GAPDH activity. In bovine aortic endothelial cells, GAPDH antisense oligonucleotides activated each of the pathways of hyperglycemic vascular damage in cells cultured in 5 mM glucose to the same extent as that induced by culturing cells in 30 mM glucose. Hyperglycemia-induced GAPDH inhibition was found to be a consequence of poly(ADP-ribosylation) of GAPDH by poly(ADP-ribose) polymerase (PARP), which was activated by DNA strand breaks produced by mitochondrial superoxide overproduction. Both the hyperglycemia-induced decrease in activity of GAPDH and its poly(ADP-ribosylation) were prevented by overexpression of either uncoupling protein-1 (UCP-1) or manganese superoxide dismutase (MnSOD), which decrease hyperglycemia-induced superoxide. Overexpression of UCP-1 or MnSOD also prevented hyperglycemia-induced DNA strand breaks and activation of PARP. Hyperglycemia-induced activation of each of the pathways of vascular damage was abolished by blocking PARP activity with the competitive PARP inhibitors PJ34 or INO-1001. Elevated glucose increased poly(ADP-ribosylation) of GAPDH in WT aortae, but not in the aortae from PARP-1-deficient mice. Thus, inhibition of PARP blocks hyperglycemia-induced activation of multiple pathways of vascular damage.

*J. Clin. Invest.* 112:1049–1057 (2003). doi:10.1172/JCI200318127.

## Introduction

Diabetes causes a variety of pathologic changes in capillaries, arteries, and peripheral nerves. Large prospective clinical studies in both type 1 and type 2 diabetic patients have shown that there is a strong relationship between the level of hyperglycemia and both the onset and progression of diabetic microvascular complications in the retina, kidney, and peripheral nerve (1, 2). Hyperglycemia also appears to have an important role in the pathogenesis of diabetic macrovascular disease (2, 3).

Received for publication February 13, 2003, and accepted in revised form July 22, 2003.

**Address correspondence to:** Michael Brownlee, Diabetes Research Center, Albert Einstein College of Medicine, 1300 Morris Park Avenue, New York, New York 10461, USA. Phone: (718) 430-3636; Fax: (718) 430-8570; E-mail: brownlee@aecom.yu.edu.

**Conflict of interest:** Csaba Szabó and Zsuzsanna Zsengellér are employees of Inotek Pharmaceuticals, a company involved in the commercial development of PARP inhibitors. Csaba Szabó is also a stockholder and director of Inotek Pharmaceuticals.

**Nonstandard abbreviations used:** advanced glycation end product (AGE); oligonucleotide (ODN); poly(ADP-ribose) polymerase (PARP); uncoupling protein-1 (UCP-1); manganese superoxide dismutase (MnSOD); bovine aortic endothelial cell (BAEC); arbitrary units (AU); reactive oxygen species (ROS).

Four major molecular mechanisms have been implicated in hyperglycemia-induced tissue damage: activation of PKC isoforms via de novo synthesis of the lipid second messenger diacylglycerol, increased hexosamine pathway flux, increased advanced glycation end product (AGE) formation, and increased polyol pathway flux. In aortic endothelial cells, hyperglycemia also activates the proinflammatory transcription factor NF- $\kappa$ B. Recently, it has been shown that all of these mechanisms reflect a single hyperglycemia-induced process: overproduction of superoxide by the mitochondrial electron transport chain (4, 5). However, the molecular mechanism by which this hyperglycemia-induced overproduction of superoxide activates these different pathways of hyperglycemic damage has not been elucidated.

Because hyperglycemia-induced overproduction of superoxide significantly inhibits GAPDH activity (6), we hypothesized that this inhibition would activate all the pathways of hyperglycemic damage by diverting upstream glycolytic metabolites into these signaling pathways. To test this hypothesis, we first evaluated the effect of inhibition of GAPDH activity by antisense oligonucleotide (ODN) on the activity of each of these pathways in aortic endothelial cells cultured in 5 mM glucose. Because aldose reductase

activity is extremely low in aortic endothelial cells, this pathway was not investigated.

We next investigated the mechanism by which hyperglycemia-induced overproduction of superoxide inhibits GAPDH activity *in vivo*. Although GAPDH activity can be inhibited by a number of covalent modifications in the *in vitro* systems, including direct oxidative modification of protein thiols, NO-dependent binding of NAD<sup>+</sup>, and mono(ADP-ribosylation) (7–9), the physiologic importance of each of these remains unclear. Because hyperglycemia-induced loss of endothelium-dependent vasodilatation can be normalized by inhibition of poly(ADP-ribose) polymerase (PARP) (10), we examined first the relationship between hyperglycemia-induced reactive oxygen formation, poly(ADP-ribosylation), and GAPDH activity. Because PARP is activated by single- or double-strand breaks in DNA, we also examined the relationship between hyperglycemia-induced reactive oxygen formation and DNA strand breaks and the consequent activation of PARP. Hyperglycemia-induced ADP-ribosylation of GAPDH was evaluated in aortae from WT and PARP-1 KO mice to determine whether this nuclear isoform of PARP is the major isoform responsible for modifying GAPDH.

Finally, we sought to determine whether this sequence of events explained the activation of pathways of hyperglycemic damage in aortic endothelial cells by examining the effect of PARP inhibition on hyperglycemia-induced activation of all these pathways in aortic endothelial cells.

## Methods

**Materials.** Eagle's MEM, nonessential amino acids, and antibiotics were from Gibco (Grand Island, New York, USA). FBS was from Hyclone (Logan, Utah, USA). Manganese (III) tetrakis(4-benzoic acid) porphyrin was from Calbiochem (La Jolla, California, USA). Fluorescent oligos used in the NF- $\kappa$ B assay were obtained from Operon Technologies Inc. (Alameda, California, USA). Monoclonal anti-poly(ADP-ribose) IgG (10H) was from Alexis (Carlsbad, California, USA). Protein A Sepharose was from Amersham Pharmacia Biotech (Piscataway, New Jersey, USA). The potent PARP inhibitors, the phenanthridinone-based PJ34 and the indeno-isoquinolinone-based INO-1001, were synthesized as previously described (11–14). Aortae from WT and PARP-deficient mice were obtained and placed into normal and high-glucose conditions as previously described (10).

**Cell culture conditions.** Confluent bovine aortic endothelial cells (BAECs) (passage 4–10) were maintained in Eagle's MEM containing 0.4% FBS, essential and nonessential amino acid, and antibiotics. Cells were incubated for 3 days before determination of PKC activity, 48 hours before determination of hexosamine pathway activity, for 5 days before determination of advanced glycation end product formation, and for 6 hours before determination of NF- $\kappa$ B

activation. Cells were infected with adenoviruses 48 hours before addition of 30 mM glucose. The final concentration of PJ34 was 3  $\mu$ M. The final concentration of INO-1001 was 300 nM.

**Oligonucleotide synthesis and treatment of cells.** Phosphorothioate oligonucleotides were synthesized by Operon Technologies Inc. The S-antisense GAPDH had the following sequence: 5'-G\*TAGAAGCAGGGATGATAT\*T-3'. Scrambled oligonucleotides (5'-G\*AATAAGTGATACGGATGT\*G-3') were used as controls.

Oligo solutions were prepared in 10 mM Tris buffer, pH 7.4, containing 1 mM EDTA, 150 mM NaCl; 36.3  $\mu$ l oligonucleotide was mixed with 16.3  $\mu$ l polyethyleneimine solution and 945  $\mu$ l media, and the solution was added to the cells for 2 hours.

**GAPDH activity.** BAECs were grown to confluence, harvested by using trypsin-EDTA after washing twice with PBS, and resuspended in lysis buffer. The cytosolic fraction was prepared by centrifuging the lysate at 100,000 *g* at 4°C for 30 minutes. Protein was measured by using the Pierce Coomassie Plus reagent (Pierce Biotechnology, Rockford, Illinois, USA). GAPDH activity was determined as described previously (6, 15).

**Adenoviral vectors.** Rat UCP-1 sense and antisense cDNAs were provided by D. Ricquier (Centre National de la Recherche Scientifique-Unité Propre 1511, Meudon, France) and human MnSOD cDNA was provided by L. Oberley (University of Iowa College of Medicine, Iowa City, Iowa, USA). The cDNAs were cloned into the shuttle vector pAd5CMV $\kappa$ -NpA and adenoviral vectors were prepared by the Gene Transfer Vector Core at the University of Iowa. Cells were infected at an MOI of 500 for 2 hours.

**Quantitation of DNA strand breaks.** DNA strand breaks were detected with a single-cell gel electrophoresis assay (CometAssay, Trevigen, Gaithersburg, Maryland, USA) according to the manufacturer's instructions. DNA strand breaks were quantitated by examining the fixed and stained cells under a fluorescence microscope (Olympus IX70; Olympus, Melville, New York, USA) with  $\times 10$  planoapo objectives. All analyses were performed with IP Lab Spectrum (Scanalytics, Fairfax, Virginia, USA). The mean length of the DNA tail was determined by measuring 40 cells for each condition.

**PARP activity.** Cells were incubated for 5 minutes at 37°C in assay buffer containing 125 nmol NAD<sup>+</sup> spiked with 0.25  $\mu$ Ci of <sup>3</sup>H-NAD<sup>+</sup> (Amersham Pharmacia Biotech) as described (16). Enzyme activity was determined by measuring cpm incorporated into protein.

**Immunoprecipitation.** BAECs were plated in 100 mm cell culture plates and grown to confluence. Cells ( $2 \times 10^7$ ) were scraped from the plates, and 500  $\mu$ g protein was immunoprecipitated with 4  $\mu$ g of the indicated antibody and 20  $\mu$ l Protein A Sepharose 4B (Amersham Pharmacia Biotech) in binding buffer (final concentration 1  $\mu$ g protein/ $\mu$ l).

For cell fractionation experiments, the cytosol fraction was obtained by centrifugation at 16,000 *g* for 10

minutes at 4°C. The cytosol fraction was aspirated, and the insoluble fraction containing the nuclei was resuspended with 200 µl nuclear extraction reagent, vortexed, and then centrifuged at 16,000 g for 10 minutes at 4°C. For in vivo immunoprecipitated Western blots, thoracic aortas from WT and PARP-deficient mice were incubated exactly as described in (10).

**Western blotting.** Immunoprecipitated proteins electrophoresed on 10% PAGE gels were transferred onto nitrocellulose membranes. The immunoblots were developed with 1:1000 dilutions of anti-poly(ADP-ribose) IgG, and the signal was detected with the ECL system according to the manufacturer's instructions (Amersham Pharmacia Biotech). The images were scanned into a Molecular Dynamics FluorImager and analyzed using the ImageQuant 5.5 program (Amersham Pharmacia Biotech).

**PKC activity.** The assay was performed according to the manufacturer's instructions using the Protein Kinase C Assay System (InVitroGen, Carlsbad, California, USA).

**Hexosamine pathway activity.** Hexosamine pathway activity was assessed by measuring UDP-GlcNAc concentration. Cells were homogenized in three volumes (600 µl) of cold 0.6 M perchloric acid and kept at 0°C for 10 minutes. The precipitated proteins were removed by centrifugation for 5 minutes at 13,500 g, and UDP-GlcNAc in the supernatant was determined by HPLC as previously described (17).

**Advanced glycation end products.** Equal amounts of cell extract protein were used for quantitative immunoblotting performed as described (18). Methylglyoxal-derived imidazole advanced glycation end products were detected using monoclonal antibody 1H7G5 at a 1:10,000 dilution. Immunocomplexes were visualized using an enhanced chemifluorescence kit according to the manufacturer's instructions (Amersham Pharmacia Biotech) and quantified using a Molecular Dynamics FluorImager and its ImageQuant 4.0 analytical software. This epitope was chosen because methylglyoxal is the principal AGE precursor induced in endothelial cells by hyperglycemia (18, 19), and the hydroimidazolone adduct is the major methylglyoxal-derived epitope (18).

**NF-κB activation.** A fluorescence in situ DNA-protein binding assay was performed in cultured cells as described (20), and fluorescence per cell was determined using IP Lab Spectrum.

**Statistics.** Data were analyzed using one-factor ANOVA to compare the means of all the groups. The Tukey-Kramer multiple comparisons procedure was used to determine which pairs of means were different.

## Results

**Specificity of GAPDH antisense ODN.** To test our hypothesis that hyperglycemia-induced mitochondrial superoxide overproduction activates pathways of hyperglycemic damage by partially inhibiting GAPDH and thereby diverting upstream glycolytic metabolites into these signaling pathways, we first needed to deter-

mine the specificity and efficacy of the GAPDH antisense ODNs. As previously reported (6), incubation of cells in 30 mM glucose reduced GAPDH activity by 73%, from  $157.9 \pm 17.6$  nmol/s/mg protein (5 mM glucose) to  $42.2 \pm 10.5$  nmol/s/mg protein (Figure 1). After transfection with GAPDH antisense, cells incubated in 5 mM glucose showed a similar reduction in GAPDH activity, from  $157.9 \pm 17.6$  nmol/s/mg protein (5 mM glucose) to  $34.3 \pm 8.8$  nmol/s/mg protein (5 mM glucose + antisense). In contrast, after transfection with GAPDH scrambled ODNs, GAPDH activity in cells incubated in 5 mM glucose was unchanged from that of cells incubated in 5 mM glucose alone ( $184.3 \pm 23.6$  nmol/s/mg protein (5 mM glucose + scrambled oligos) versus  $157.9 \pm 17.6$  nmol/s/mg protein (5 mM glucose alone). That this reduction in activity by GAPDH antisense reflected a decrease in GAPDH protein was confirmed by immunoblotting (data not shown).

**Effect of GAPDH antisense ODN on PKC activation, hexosamine pathway activation, intracellular AGE formation, and NF-κB activation in cells cultured in 5 mM glucose.** Incubation of bovine aortic endothelial cells with 30 mM glucose increased the membrane fraction of intracellular PKC activity from  $104.45 \pm 10.06$  pmol/min/mg protein in cells incubated in 5 mM glucose (Figure 2a, bar 1) to  $224.54 \pm 23.94$  pmol/min/mg protein (Figure 2a, bar 2), as previously described (5). After transfection with GAPDH antisense (Figure 2a, bar 3), cells incubated in 5 mM glucose showed a similar increase in PKC activity, from  $104.45 \pm 10.06$  pmol/min/mg protein (5 mM glucose) to  $196.63 \pm 11.09$  pmol/min/mg protein (5 mM glucose + antisense). In contrast, after transfection with GAPDH scrambled ODNs (Figure 2a, bar 4), PKC activity in cells incubated in 5 mM glucose was unchanged from that of cells incubated in 5 mM glucose alone  $81.13 \pm 13.18$  pmol/min/mg protein (5 mM glucose + scrambled ODN) versus  $104.45 \pm 10.06$  pmol/min/mg protein (5 mM glucose alone).

Similarly, incubation of BAECs with 30 mM glucose increased the UDP-N-acetylglucosamine concentration, an indicator of hexosamine pathway flux, from

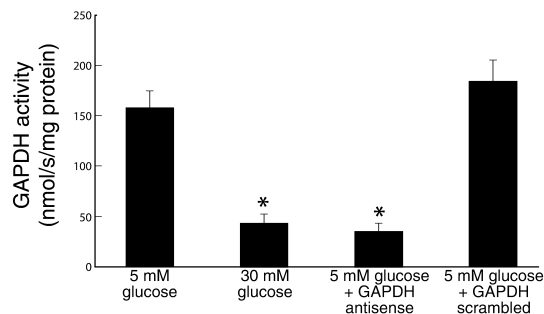


**Figure 1** Effect of GAPDH antisense ODNs on GAPDH activity in BAECs. Each bar represents the mean ± SEM of four separate experiments. \* $P < 0.01$  compared with cells incubated in 5 mM glucose alone.

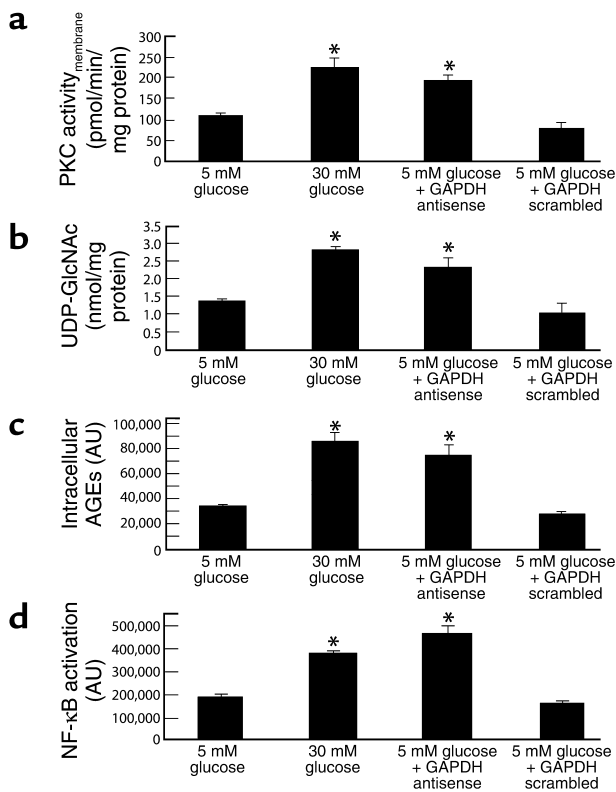


**Figure 2**  
Effect of GAPDH antisense ODNs on pathways of hyperglycemic damage in BAECs. (a) PKC activation; (b) hexosamine pathway activation; (c) intracellular AGE formation; (d) NF-κB activation. \* $P < 0.01$  compared with cells incubated in 5 mM glucose. AU, arbitrary units. For a through c, each bar represents the mean  $\pm$  SEM of four separate experiments. For d, each bar represents the mean  $\pm$  SEM of fluorescence from 40 cells measured in an in situ DNA-protein binding assay.

1.35  $\pm$  0.08 nmol/mg protein in cells incubated with 5 mM glucose (Figure 2b, bar 1) to 2.82  $\pm$  0.12 nmol/mg protein (Figure 2b, bar 2), as previously described (6). After transfection with GAPDH antisense (Figure 2b, bar 3), cells incubated in 5 mM glucose showed a similar increase in UDP-N-acetylglucosamine, from 1.35  $\pm$  0.08 nmol/mg protein (5 mM glucose) to 2.38  $\pm$  0.30 nmol/mg protein (5 mM glucose + antisense). In contrast, after transfection with GAPDH scrambled ODNs (Figure 2a, bar 4), UDP-N-acetylglucosamine concentration in cells incubated in 5 mM glucose was unchanged from that of cells incubated in 5 mM glucose alone, 1.06  $\pm$  0.03 nmol/mg protein (5 mM glucose + scrambled ODN) versus 1.35  $\pm$  0.08 nmol/mg protein (5 mM glucose alone).

Incubation of BAECs with 30 mM glucose increased intracellular AGE formation from 33,315  $\pm$  1,750 arbitrary units (AU) in cells incubated in 5 mM glucose (Figure 2c, bar 1) to 85,954  $\pm$  7,431 AU (Figure 2c, bar 2), as previously described (5). This hyperglycemia-induced 2.6-fold increase was reproduced in cells transfected with GAPDH antisense (Figure 2c, bar 3) (74,837  $\pm$  3,828 AU), whereas in cells transfected with GAPDH scrambled ODN (Figure 2c, bar 4), AGE for-

mation was not different (27,238  $\pm$  3,819 AU) from that of cells incubated in 5 mM glucose alone.

Lastly, incubation of BAECs with 30 mM glucose increased NF-κB activation by twofold, from 188,636  $\pm$  13,333 AU in cells incubated in 5 mM glucose (Figure 2d, bar 1) to 379,053  $\pm$  9,734 AU in cells incubated in 30 mM glucose (Figure 2d, bar 2), as previously described (5). This hyperglycemia-induced increase was reproduced in cells transfected with GAPDH antisense (Figure 2d, bar 3) (465,044  $\pm$  31,474 AU), whereas in cells transfected with GAPDH scrambled ODN (Figure 2d, bar 4), NF-κB activation was not increased (160,009  $\pm$  13,388 AU) above that of cells incubated in 5 mM glucose alone.

*Effect of PARP inhibition on GAPDH activity.* We next evaluated the extent of poly(ADP-ribosylation) on GAPDH in BAECs. Immunoprecipitation of GAPDH, followed by Western blotting with anti-poly(ADP-ribose) IgG showed that incubation of cells in 30 mM glucose increased covalent modification of GAPDH by 2.2-fold, from 57,155  $\pm$  5,288 AU (Figure 3a, bar 1) to 125,532  $\pm$  9,577 AU (Figure 3a, bar 2). This increased modification of GAPDH by poly(ADP-ribosylation) was completely prevented in cells exposed to 30 mM glucose by overexpression of either UCP-1 (Figure 3a, bar 4), a specific protein uncoupler of oxidative phosphorylation capable of collapsing the proton electrochemical gradient that drives superoxide production (5), or MnSOD (21), the mitochondrial isoform of this enzyme (Figure 3a, bar 5). The poly(ADP-ribosylation) of GAPDH induced by 30 mM glucose was also completely prevented by addition of the potent PARP inhibitor, PJ34 (Figure 3a, bar 6).

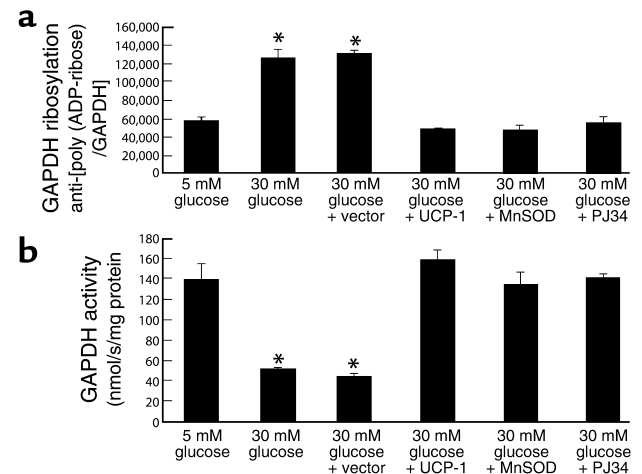


**Figure 3**  
Effect of genes that alter mitochondrial superoxide production and of PARP inhibition on poly(ADP-ribosylation) of GAPDH (a), and on GAPDH activity (b), in BAECs. Cells were incubated in 5 mM glucose or 30 mM glucose alone, in 30 mM glucose plus either control, UCP-1- or MnSOD-expressing adenoviral vectors, and in 30 mM glucose plus 3  $\mu$ M PJ34. Each bar represents the mean  $\pm$  SEM of four separate experiments. \* $P < 0.01$  compared with cells incubated in 5 mM glucose alone.

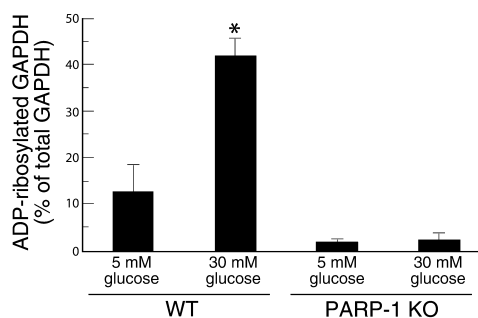


**Figure 4**  
Effect of hyperglycemia on poly(ADP-ribosyl)ation of GAPDH in aortas from WT and PARP-1 KO mice. Each bar represents the mean  $\pm$  SEM of four separate experiments. \* $P < 0.01$  compared with aortas incubated in 5 mM glucose.

We then assessed the effect of this covalent modification on GAPDH activity (Figure 3b). As described previously (6), the inhibitory effect of incubation in 30 mM glucose was completely prevented by overexpression of either UCP-1 (Figure 3b, bar 4) or MnSOD (Figure 3b, bar 5), in parallel with the changes in poly(ADP-ribosyl)ation of GAPDH. The prevention of hyperglycemia-induced inhibition of GAPDH activity by PJ34 (Figure 3b, bar 6) directly demonstrated that hyperglycemia-induced overproduction of superoxide-inhibited GAPDH activity by causing poly(ADP-ribosyl)ation of the enzyme via PARP. Because PARP is exclusively in the nucleus, we examined the subcellular distribution of both poly(ADP-ribosyl)ated and unmodified GAPDH. In response to 30 mM glucose, there was a 1.7-fold increase of GAPDH modification in both the cytoplasmic and nuclear compartments, whereas the unmodified GAPDH decreased 64% in cytoplasm and 27% in the nucleus (data not shown). Approximately 60% of the poly(ADP-ribosyl)ated GAPDH was in the nucleus, and 40% in the cytoplasm, both in cells exposed to 30 mM glucose, and in cells exposed to 5 mM glucose (data not shown).

Treatment of the cells with a second, structurally unrelated PARP inhibitor, INO-1001 (300 nM), yielded results identical to those seen with PJ34 (data not shown). These data are consistent with an unaltered translocation of modified GAPDH from the nuclear compartment to the cytosolic compartment. In vivo, aortas from *PARP-1* KO mice (10) showed no increase in GAPDH poly(ADP-ribosyl)ation after incubation in high glucose, whereas aortas from WT mice showed a nearly fourfold increase (Figure 4).

**Effect of hyperglycemia-induced mitochondrial superoxide overproduction on PARP activity.** To confirm directly that hyperglycemia-induced mitochondrial superoxide overproduction activated PARP, activity of this enzyme was determined (Figure 5). Incubation of BAECs in 30 mM glucose increased PARP activity 1.7-fold, from  $147.5 \pm 4.7$  pmol/min/mg protein in cells incubated with 5 mM glucose (Figure 5, bar 1) to

$254.9 \pm 15.6$  pmol/min/mg protein (Figure 5, bar 2). The activation of PARP by 30 mM glucose was completely inhibited by overexpression of either UCP-1 (Figure 5, bar 4) or MnSOD (Figure 5, bar 5) to  $152.1 \pm 15.1$  pmol/min/mg protein and  $165.5 \pm 9.5$  pmol/min/mg protein, respectively, whereas vector alone had no effect.

**Effect of hyperglycemia-induced mitochondrial superoxide overproduction on DNA strand breaks.** Because PARP is activated by single- or double-strand breaks in DNA (22), the effect of hyperglycemia-induced mitochondrial superoxide overproduction on DNA strand breaks was determined using the COMET single-cell electrophoresis assay (Figure 6). Incubation in 30 mM glucose increased the length of the DNA tail twofold, compared to 5 mM glucose, from  $13.65 \pm 0.76$   $\mu$ m (Figure 6, a and f, bar 1) to  $30.99 \pm 0.7$   $\mu$ m (Figure 6, b and f, bar 2). The increase in DNA strand breaks induced by 30 mM glucose was completely inhibited by overexpression of either UCP-1 (Figure 6, d and f, bar 4) or MnSOD (Figure 6, e and f, bar 5) to  $15.67 \pm 0.77$   $\mu$ m and  $18.27 \pm 0.57$   $\mu$ m, respectively, whereas vector alone had no effect (Figure 6, c and f, bar 3).

**Effect of PARP inhibition on PKC activation, hexosamine pathway activation, intracellular AGE formation, and NF- $\kappa$ B activation in cells cultured in 30 mM glucose.** Having demonstrated that hyperglycemia-induced mitochondrial superoxide overproduction inhibits GAPDH activity by PARP-mediated poly(ADP-ribosyl)ation of the enzyme as a result of reactive oxygen species-induced (ROS-induced) DNA strand breaks, and having shown that inhibiting GAPDH with antisense ODN activates multiple pathways of hyperglycemic damage in cells cultured in 5 mM glucose to the same extent as does culturing these cells in 30 mM glucose, we sought to determine whether this sequence of events explained the activation of these

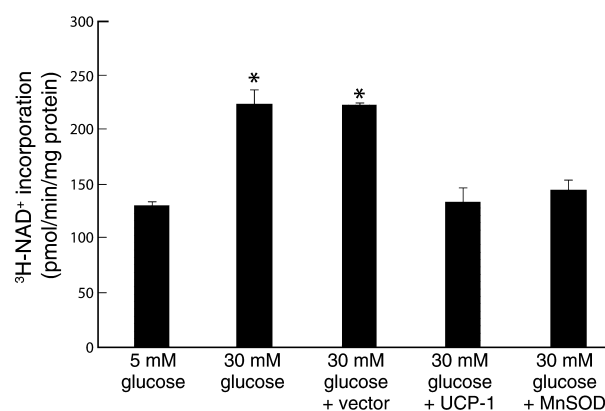


**Figure 5**  
Effect of hyperglycemia and genes that alter mitochondrial superoxide production on PARP activity in BAECs. Cells were incubated in 5 mM glucose or 30 mM glucose alone, in 30 mM glucose plus either control, UCP-1- or MnSOD-expressing adenoviral vectors, and in 30 mM glucose plus 3  $\mu$ M PJ34. Each bar represents the mean  $\pm$  SEM of four separate experiments. \* $P < 0.01$  compared with cells incubated in 5 mM glucose alone.

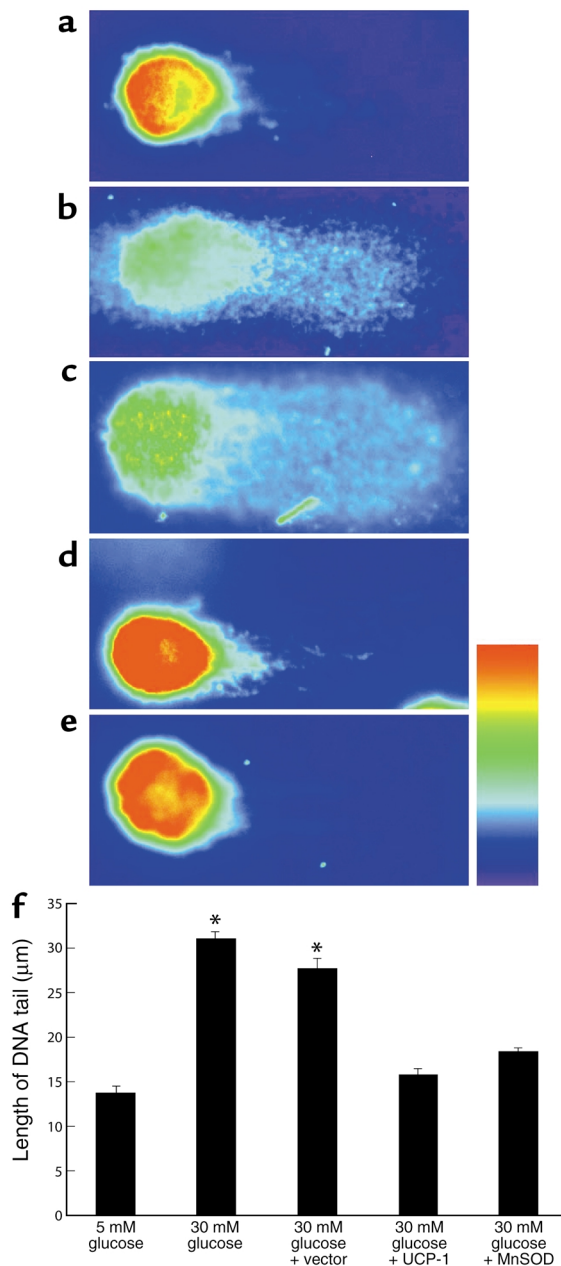


**Figure 6** Effect of hyperglycemia and genes that alter mitochondrial superoxide production on DNA strand breaks in BAECs. Cells were incubated in 5 mM glucose (a) or 30 mM glucose alone (b), or in 30 mM glucose plus either control (c), UCP-1-expressing (d) or MnSOD-expressing (e) adenoviral vectors. Fluorescent micrographs from single-cell electrophoresis assay. (f) Quantitation of DNA strand breaks from single-cell electrophoresis assay. Each bar represents the mean  $\pm$  SEM of 40 cells for each incubation condition. \* $P < 0.01$  compared with cells incubated in 5 mM glucose alone.

of BAECs with 30 mM glucose increased the UDP-N-acetylglucosamine concentration, an indicator of hexosamine pathway flux from  $1.18 \pm 0.13$  nmol/mg protein in cells incubated with 5 mM glucose (Figure 7b, bar 1) to  $2.4 \pm 0.3$  nmol/mg protein (Figure 7b, bar 2). Overexpression of either UCP-1 or MnSOD completely inhibited the effect of 30 mM glucose to  $1.2 \pm 0.1$  nmol/mg protein and  $1.2 \pm 0.2$  nmol/mg protein, respectively (Figure 7b, bars 4 and 5), as shown previously (6). Inhibition of PARP by PJ34 also completely prevented the effect of 30 mM glucose (Figure 7b, bar 6). Incubation of BAECs with 30 mM glucose also increased intracellular AGE formation from  $58,107 \pm 3,765$  AU in cells incubated in 5 mM glucose (Figure 7c, bar 1) to  $92,707 \pm 12,906$  AU (Figure 7c, bar 2). Overexpression of either UCP-1 or MnSOD completely inhibited the effect of 30 mM glucose to  $56,527 \pm 6,319$  AU and  $48,094 \pm 8,739$  AU, respectively (Figure 7c, bars 4 and 5), as shown previously (5). Inhibition of PARP by PJ34 also completely prevented the effect of 30 mM glucose (Figure 7c, bar 6).

Lastly, incubation of BAECs with 30 mM glucose increased NF- $\kappa$ B activation by 2.6-fold, from  $1014 \pm 12$  AU in cells incubated in 5 mM glucose (Figure 7d, bar 1) to  $2653 \pm 40$  AU in cells incubated in 30 mM glucose (Figure 7d, bar 2). Overexpression of either UCP-1 or MnSOD completely inhibited the effect of 30 mM glucose to  $997 \pm 4.9$  AU and  $798 \pm 3.8$  AU, respectively (Figure 7d, bars 4 and 5), as shown previously (5). Inhibition of PARP by PJ34 also completely prevented this effect of 30 mM glucose (Figure 7d, bar 6). PJ34, unlike earlier generation PARP inhibitors, has no antioxidant properties and acts by competitive blockade of the NAD<sup>+</sup> binding site in the enzyme. Nevertheless, to further verify that the observed effects were due to PARP inhibition, a structurally unrelated PARP inhibitor, INO-1001, was used. The effects of INO-1001 on hyperglycemia-induced PKC activation and NF- $\kappa$ B activation were identical to those with PJ34 (data not shown).

### Discussion

Four major hypotheses about how hyperglycemia causes diabetic complications have generated a large amount of data, as well as several clinical trials that were based on specific inhibitors of these mechanisms. The four hypotheses are activation of PKC isoforms, increased hexosamine pathway flux, increased

pathways by hyperglycemia in vivo (Figure 7). We therefore evaluated the effect of PARP inhibition by PJ34 on each of the pathways of hyperglycemic damage in cells incubated with 30 mM glucose.

Incubation of BAECs in 30 mM glucose increased the membrane fraction of intracellular PKC activity from  $123.79 \pm 17.3$  pmol/min/mg protein in cells incubated in 5 mM glucose (Figure 7a, bar 1) to  $280.14 \pm 6.52$  pmol/min/mg protein (Figure 7a, bar 2). Overexpression of either UCP-1 or MnSOD completely inhibited the effect of 30 mM glucose to  $75.6 \pm 28.1$  pmol/min/mg protein and  $107.15 \pm 19.9$  pmol/min/mg, respectively (Figure 7a, bars 4 and 5), as shown previously (5). Inhibition of PARP by PJ34 also completely prevented the activation of PKC by 30 mM glucose (Figure 7a, bar 6). Similarly, incubation

AGE formation, and increased polyol pathway flux. Although specific inhibitors of individual pathways each ameliorate or prevent various diabetes-induced functional and structural abnormalities in cell culture and animal models, there has been no apparent common element linking the four mechanisms of hyperglycemia-induced damage (23–27). This issue has now been resolved by the recent discovery that each of the four different pathogenic mechanisms reflects a single hyperglycemia-induced process: overproduction of superoxide by the mitochondrial electron transport chain (4, 5).

In this report, we show that hyperglycemia-induced overproduction of superoxide by the mitochondrial electron transport chain activates the three major pathways of hyperglycemic damage found in aortic endothelial cells (activation of PKC isoforms, hexosamine pathway flux, and AGE formation) by inhibiting GAPDH activity. Inhibition of GAPDH activity also activates the proinflammatory transcription factor NF- $\kappa$ B, which in aortic endothelial cells is PKC dependent (4, 28). This GAPDH inhibition is a consequence of poly(ADP-ribosylation) of GAPDH by PARP, which is activated by DNA strand breaks produced by mitochondrial superoxide overproduction. Hyperglycemia-induced activation of each of these pathways is completely inhibited by blocking PARP activity with two structurally unrelated PARP inhibitors.

Recent evidence has shown that GAPDH is not simply a classical glycolytic enzyme. Instead, it is a multifunctional protein with diverse cytoplasmic, membrane, and nuclear activities (29, 30). It is important to note that antisense ODNs can occasionally affect transcription of additional genes, so it is theoretically possible that the GAPDH antisense experiments reflect a different effect than reduction of GAPDH activity, perhaps resulting in reduced translocation of GAPDH from the nucleus. However, because restoration of GAPDH activity by inhibition of PARP blocks the effects observed in the GAPDH antisense experiments, this possibility is unlikely, and GAPDH antisense ODNs reduced GAPDH protein content proportionally (data not shown). In response to hyperglycemia, there was a 1.7-fold increase in GAPDH poly(ADP-ribosylation) in both compartments. In vivo, aortas from *PARP-1* KO mice showed no increase in GAPDH poly(ADP-ribosylation) after incubation in high glucose, whereas aortas from WT mice showed a nearly fourfold increase, thus demonstrating that the nuclear PARP isoform, PARP-1, was exclusively responsible for GAPDH poly(ADP-ribosylation).

During cell death, GAPDH translocates into the nucleus (31, 32), and recent work demonstrated that GAPDH can form complexes with nuclear proteins (33). Various modifications of the enzyme have been described, including its mono(ADP-ribosylation) by NO (34). Here, using a combination of immunohistochemical and pharmacologic tools, we demonstrate the

poly(ADP-ribosylation) of the enzyme, which is likely to occur in association with its nuclear translocation.

PARP is a nuclear DNA-repair enzyme that is activated by DNA strand breaks. Once activated, PARP catalyzes attachment of ADP-ribose units from NAD<sup>+</sup> to nuclear proteins, cleaving NAD<sup>+</sup> into its component parts, ADP-ribose and nicotinamide mononucleotide. Replacement of this PARP-induced depletion of NAD<sup>+</sup> consumes ATP. When PARP activation is excessive, this ATP consumption can cause cell death due to energy deficit (35). PARP-1 poly(ADP-ribosylates) transcription factors such as p53 and fos (36). However, PARP may also act as a coactivator or repressor of other transcription factors independent of its catalytic activity (36). Neither the enzymatic nor the DNA binding activity of PARP-1 is required for NF- $\kappa$ B coactivator function (36, 37), for example, and PARP activity inhibitors fail to suppress inflammation-induced pro-IL-1 $\beta$  and ICAM-1 expression, whereas deletion of the *PARP-1* gene does.

Thus, although mice lacking the *PARP* gene are resistant to injury from cerebral ischemia (35) and

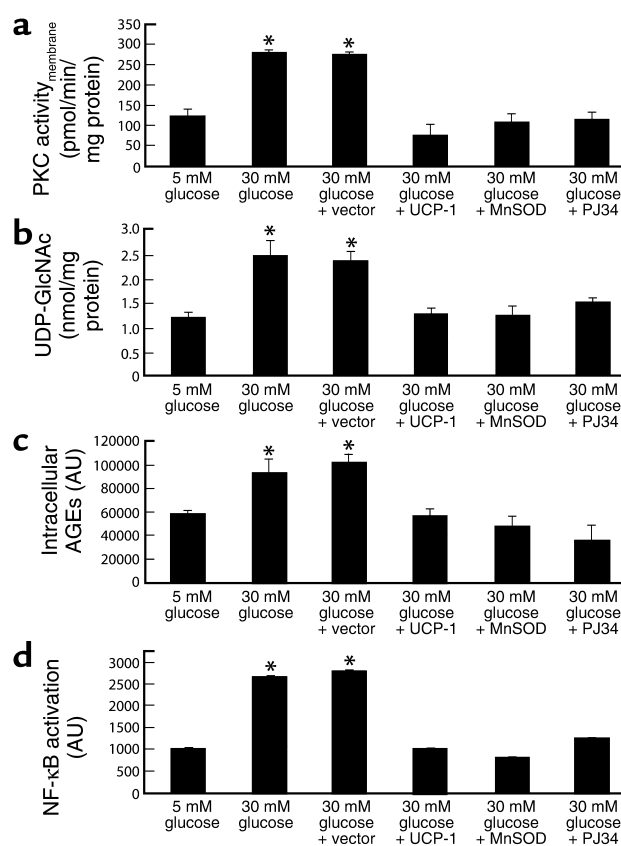


**Figure 7** Effect of PARP inhibition on hyperglycemia-induced pathways of vascular damage in BAECs. (a) PKC activation; (b) hexosamine pathway activation; (c) intracellular AGE formation; (d) NF- $\kappa$ B activation. \* $P < 0.01$  compared with cells incubated in 5 mM glucose. For a through c, each bar represents the mean  $\pm$  SEM of four separate experiments. For d, each bar represents the mean  $\pm$  SEM of fluorescence from 40 cells measured in an in situ DNA-protein binding assay.

myocardial ischemia-reperfusion (38), it is not known whether these effects are due to altered PARP enzymatic activity or to altered protein-protein interactions with PARP. Hyperglycemia-induced NF- $\kappa$ B activation does not occur in pulmonary microvascular endothelial cells of PARP-deficient mice, for example, whereas inhibition of PARP activity in WT pulmonary microvascular endothelial cells has no effect on hyperglycemia-induced NF- $\kappa$ B activation (10). In diabetic animal models, PARP inhibitors have been shown to improve myocardial dysfunction (39) and to prevent and reverse hyperglycemia-induced loss of endothelium-dependent vasodilatation (39, 40). Although PKC activation has been implicated in diabetic myocardial dysfunction (41), and both PKC and the hexosamine pathway have been implicated in hyperglycemia-induced loss of endothelium-dependent vasodilatation (42, 43), a possible link between PARP inhibition and activity of these pathways has not been investigated previously. Because there are two distinct mechanisms by which PARP affects cell function, poly(ADP-ribosylation) and protein-protein interaction, it has not been possible to predict whether PARP inhibition would have any effect on the development of long-term diabetic complications.

In animal models of long-term diabetic complications, it has been shown that treatment with a  $\beta$  isoform-specific PKC inhibitor ameliorates glomerular mesangial expansion (44), the pathognomonic structural feature of diabetic renal complications. It has also been shown that treatment of diabetic animal models with AGE inhibitors partially prevents various functional and structural manifestations of diabetic microvascular disease in retina, kidney, and nerve (23, 26, 27) and that blockade of the AGE receptor in diabetic apoE-null mice significantly reduces atherosclerotic lesion size and structure (45, 46). Inhibition of both these pathways by the lipid-soluble thiamine derivative benfotiamine also prevents the development of experimental diabetic retinopathy (19). The demonstration in this report that inhibition of PARP completely blocks hyperglycemia-induced activation of both of these pathways suggests that PARP inhibitors might have unique clinical efficacy in preventing the development and progression of diabetic complications.

### Acknowledgments

We thank the Diabetes Research and Training Center of the Albert Einstein College of Medicine for performing analyses of UDP-N-acetylglucosamine. This work was supported in part by grants from the NIH and the American Diabetes Association.

1. The Diabetes Control and Complications Trial Research Group. 1993. The effect of intensive treatment of diabetes on the development and progression of long-term complications in insulin-dependent diabetes mellitus. The Diabetes Control and Complications Trial Research Group. *N. Eng. J. Med.* **329**:977–986.
2. UK Prospective Diabetes Study (UKPDS) Group. 1998. Intensive blood-glucose control with sulphonylureas or insulin compared with conventional

- treatment and risk of complications in patients with type 2 diabetes (UKPDS 33). UK Prospective Diabetes Study (UKPDS) Group. *Lancet.* **352**:837–853.
3. Wei, M., Gaskill, S.P., Haffner, S.M., and Stem, M.P. 1998. Effects of diabetes and level of glycemia on all-cause and cardiovascular mortality. The San Antonio Heart Study. *Diabetes Care.* **21**:1167–1172.
  4. Brownlee, M. 2001. Biochemistry and molecular cell biology of diabetic complications. *Nature.* **414**:813–820.
  5. Nishikawa, T., et al. 2000. Normalizing mitochondrial superoxide production blocks three pathways of hyperglycaemic damage. *Nature.* **404**:787–790.
  6. Du, X.L., et al. 2000. Hyperglycemia-induced mitochondrial superoxide overproduction activates the hexosamine pathway and induces plasminogen activator inhibitor-1 expression by increasing Sp 1 glycosylation. *Proc. Natl. Acad. Sci. U. S. A.* **97**:12222–12226.
  7. Molina y Vedia, L., et al. 1992. Nitric oxide-induced S-nitrosylation of glyceraldehyde-3-phosphate dehydrogenase inhibits enzymatic activity and increases endogenous ADP-ribosylation. *J. Biol. Chem.* **267**:24929–24932.
  8. McDonald, L.J., and Moss, J. 1993. Stimulation by nitric oxide of an NAD linkage to glyceraldehyde-3-phosphate dehydrogenase. *Proc. Natl. Acad. Sci. U. S. A.* **90**:6238–6241.
  9. Brune, B., and Lapetina, E.G. 1995. Protein thiol modification of glyceraldehyde-3-phosphate dehydrogenase as a target for nitric oxide signaling. *Genet. Eng. (N. Y.).* **17**:149–164.
  10. Garcia, S.F., et al. 2001. Diabetic endothelial dysfunction: the role of poly (ADP-ribose) polymerase activation. *Nat. Med.* **7**:108–113.
  11. Mabley, J.G., et al. 2001. Anti-inflammatory effects of a novel, potent inhibitor of poly (ADP-ribose) polymerase. *Inflamm. Res.* **50**:561–569.
  12. Jagtap, P., et al. 2002. Novel phenanthridinone inhibitors of poly (adenosine 5'-diphosphate-ribose) synthetase: potent cytoprotective and anti-shock agents. *Crit. Care Med.* **30**:1071–1082.
  13. Shimoda, K., et al. 2003. Effect of poly (ADP-ribose) synthetase inhibition on burn and smoke inhalation injury in the sheep. *Am. J. Physiol. Lung Cell. Mol. Physiol.* **285**:L240–L249.
  14. Khan, T.A., et al. 2003. Poly(ADP-ribose) synthetase inhibition improves postischemic myocardial function after cardioplegia-cardiopulmonary bypass. *J. Am. Coll. Surg.* **197**:270–277.
  15. Tao, Y., Howlett, A., and Klein, C. 1994. Nitric oxide regulation of glyceraldehyde-3-phosphate dehydrogenase activity in Dictyostelium discoideum cells and lysates. *Eur. J. Biochem.* **224**:447–454.
  16. Schraufstatter, I.U., Hinshaw, D.B., Hyslop, P.A., Spragg, R.G., and Cochrane, C.G. 1986. Oxidant injury of cells. DNA strand-breaks activate polyadenosine diphosphate-ribose polymerase and lead to depletion of nicotinamide adenine dinucleotide. *J. Clin. Invest.* **77**:1312–1320.
  17. Rossetti, L., and Hu, M. 1993. Skeletal muscle glycogenolysis is more sensitive to insulin than is glucose transport/phosphorylation. Relation to the insulin-mediated inhibition of hepatic glucose production. *J. Clin. Invest.* **92**:2963–2974.
  18. Shinohara, M., et al. 1998. Overexpression of glyoxalase-I in bovine endothelial cells inhibits intracellular advanced glycation endproduct formation and prevents hyperglycemia-induced increases in macromolecular endocytosis. *J. Clin. Invest.* **101**:1142–1147.
  19. Hammes, H.P., et al. 2003. Benfotiamine blocks three major pathways of hyperglycemic damage and prevents experimental diabetic retinopathy. *Nat. Med.* **9**:294–299.
  20. Kurose, I., et al. 1997. CD18/ICAM-1-dependent oxidative NF- $\kappa$ B activation leading to nitric oxide production in rat Kupffer cells cocultured with syngeneic hepatoma cells. *J. Clin. Invest.* **99**:867–878.
  21. Manna, S.K., Zhang, H.J., Yan, T., Oberley, L.W., and Aggarwal, B.B. 1998. Overexpression of manganese superoxide dismutase suppresses tumor necrosis factor-induced apoptosis and activation of nuclear transcription factor- $\kappa$ B and activated protein-1. *J. Biol. Chem.* **273**:13245–13254.
  22. Virag, L., and Szabo, C. 2002. The therapeutic potential of poly(ADP-ribose) polymerase inhibitors. *Pharmacol. Rev.* **54**:375–429.
  23. Hammes, H.P., Martin, S., Federlin, K., Geisen, K., and Brownlee, M. 1991. Aminoguanidine treatment inhibits the development of experimental diabetic retinopathy. *Proc. Natl. Acad. Sci. U. S. A.* **88**:11555–11558.
  24. Ishii, H., et al. 1996. Amelioration of vascular dysfunctions in diabetic rats by an oral PKC beta inhibitor. *Science.* **272**:728–731.
  25. Lee, A.Y., Chung, S.K., and Chung, S.S. 1995. Demonstration that polyol accumulation is responsible for diabetic cataract by the use of transgenic mice expressing the aldose reductase gene in the lens. *Proc. Natl. Acad. Sci. U. S. A.* **92**:2780–2784.
  26. Nakamura, S., et al. 1997. Progression of nephropathy in spontaneous diabetic rats is prevented by OPB-9195, a novel inhibitor of advanced glycation. *Diabetes.* **46**:895–899.
  27. Soulis-Liparota, T., Cooper, M., Papazoglou, D., Clarke, B., and Jerums, G. 1991. Retardation by aminoguanidine of development of albuminuria, mesangial expansion, and tissue fluorescence in streptozocin-induced diabetic rat. *Diabetes.* **40**:1328–1334.
  28. Pieper, G.M., and Riaz-ul-Haq. 1997. Activation of nuclear factor- $\kappa$ B in

- cultured endothelial cells by increased glucose concentration: prevention by calphostin C. *J. Cardiovasc. Pharmacol.* **30**:528–532.
29. Sirover, M.A. 1997. Role of the glycolytic protein, glyceraldehyde-3-phosphate dehydrogenase, in normal cell function and in cell pathology. *J. Cell. Biochem.* **66**:133–140.
  30. Mazzola, J.L., and Sirover, M.A. 2002. Alteration of intracellular structure and function of glyceraldehyde-3-phosphate dehydrogenase: a common phenotype of neurodegenerative disorders? *Neurotoxicology.* **23**:603–609.
  31. Sawa, A. 1997. Glyceraldehyde-3-phosphate dehydrogenase: nuclear translocation participates in neuronal and nonneuronal cell death. *Proc. Natl. Acad. Sci. U. S. A.* **94**:11669–11674.
  32. Schmitz, H.D. 2001. Reversible nuclear translocation of glyceraldehyde-3-phosphate dehydrogenase upon serum depletion. *Eur. J. Cell. Biol.* **80**:419–427.
  33. Krynetski, E.Y. et al. 2003. A nuclear protein complex containing high mobility group proteins B1 and B2, heat shock cognate protein 70, ERp60, and glyceraldehyde-3-phosphate dehydrogenase is involved in the cytotoxic response to DNA modified by incorporation of anticancer nucleoside analogues. *Cancer Res.* **63**:100–106.
  34. Brune, B., and Lapetina, E.G. 1996. Nitric oxide-induced covalent modification of glycolytic enzyme glyceraldehyde-3-phosphate dehydrogenase. *Methods Enzymol.* **269**:400–407.
  35. Eliasson, M.J., et al. 1997. Poly (ADP-ribose) polymerase gene disruption renders mice resistant to cerebral ischemia. *Nat. Med.* **3**:1089–1095.
  36. Ha, H.C., Hester, L.D., and Snyder, S.H. 2002. Poly (ADP-ribose) polymerase-1 dependence of stress-induced transcription factors and associated gene expression in glia. *Proc. Natl. Acad. Sci. U. S. A.* **99**:3270–3275.
  37. Hassa, P.O., Covic, M., Hasan, S., Imhof, R., and Hottiger, M.O. 2001. The enzymatic and DNA binding activity of PARP-1 are not required for NF- $\kappa$ B coactivator function. *J. Biol. Chem.* **276**:45588–45597.
  38. Pieper, A.A., et al. 2000. Myocardial postischemic injury is reduced by polyADPribose polymerase-1 gene disruption. *Mol. Med.* **6**:271–282.
  39. Pacher, P., et al. 2002. The role of poly (ADP-ribose) polymerase activation in the development of myocardial and endothelial dysfunction in diabetes. *Diabetes.* **51**:514–521.
  40. Soriano, F.G., Pacher, P., Mabley, J., Liaudet, L., and Szabo, C. 2001. Rapid reversal of the diabetic endothelial dysfunction by pharmacological inhibition of poly (ADP-ribose) polymerase. *Circ. Res.* **89**:684–691.
  41. Wakasaki, H., et al. 1997. Targeted overexpression of protein kinase C beta2 isoform in myocardium causes cardiomyopathy. *Proc. Natl. Acad. Sci. U. S. A.* **94**:9320–9325.
  42. Beckman, J.A., Goldfine, A.B., Gordon, M.B., Garrett, L.A., and Creager, M.A. 2002. Inhibition of protein kinase C beta prevents impaired endothelium-dependent vasodilation caused by hyperglycemia in humans. *Circ. Res.* **90**:107–111.
  43. Du, X.L., et al. 2001. Hyperglycemia inhibits endothelial nitric oxide synthase activity by posttranslational modification at the Akt site. *J. Clin. Invest.* **108**:1341–1348. doi:10.1172/JCI200111235.
  44. Koya, D., et al. 2000. Amelioration of accelerated diabetic mesangial expansion by treatment with a PKC beta inhibitor in diabetic db/db mice, a rodent model for type 2 diabetes. *FASEB J.* **14**:439–447.
  45. Bucciarelli, L.G., et al. 2002. RAGE blockade stabilizes established atherosclerosis in diabetic apolipoprotein E-null mice. *Circulation.* **106**:2827–2835.
  46. Park, L., et al. 1998. Suppression of accelerated diabetic atherosclerosis by the soluble receptor for advanced glycation endproducts. *Nat. Med.* **4**:1025–1031.